

Quadrupole Ion Traps

Localising Charged Particles by Electric and Magnetic Fields

Pushpa M Rao, Richard D'Souza and S A Ahmad



Puspha M Rao is a senior scientist at the Spectroscopy Division, BARC. She has been working in the field of high resolution atomic spectroscopy.



Richard D'Souza is a senior scientist at the Spectroscopy Division, BARC. He is presently working in the field of atomic physics.



S A Ahmad, ex-head, Atomic Spectroscopy Section, continues interaction at BARC, in studies of nuclear effects in atomic spectra, multiphoton ionisation of atoms, ion trapping & laser cooling and trapping of atoms.

During the last two decades there has been tremendous progress in the technique of trapping and cooling ions using quadrupole ion traps. Using these trapping techniques one can have charged particles of a single species confined near the trap centre, which enables to carry out studies of these ions in a well-controlled environment. The long storage times of the ions, possible in these traps, results in the elimination of transit-time broadening making it possible to do precision spectroscopic measurements on these ions. Several important experiments with single electron or ion have been undertaken to address problems related to basic physics, such as the measurement of the electron radius, precision measurements of fundamental parameters and tests of the predictions of quantum mechanics.

Introduction

Wolfgang Paul was awarded the 1989 Nobel Prize in Physics for his immense contributions to the physics and techniques of ion trappings, and in the Nobel Lecture delivered on 8th December, 1989 he said "Experimental physics is the art of observing the structure of matter and of detecting the dynamic processes within it". However, in order to understand the complicated behaviour of some natural processes, one has to measure the relevant parameters involving the matter-light interaction as precisely as possible. Measurements of atomic characteristics like energy levels of an atom or probability of transition between these levels is usually performed on a collection of atoms. Furthermore, effects such as collisions complicate and modify the values of the parameters relevant for understanding the physics of the atom. However in certain studies it is necessary to carry

out investigations on an isolated single atom/ion. Such studies have been carried out recently, resulting in some exciting observations in the field of the interaction of radiation with atoms.

A single atom at rest in free space, free of uncontrolled perturbations, would be the ideal dream of any atomic physicist. Ion traps have almost fulfilled this dream: Observation of a single atomic ion, almost at rest in a nearly perturbation-free environment, over a long period of time has become a practical reality.

The idea of trapping charged particles developed from studies on electrical discharges and has continuously evolved from extensive research in the fields of mass filters and particle accelerators. Investigation of the properties of an electrical discharge between a very thin filament cathode and a cylindrical anode led to the earliest trap called the Kingdon trap in honour of K H Kingdon. Study of the properties of the electrical discharges between coaxial cylinders in the presence of an axial magnetic field by F M Penning in 1936 led to the development of the Penning trap. The important result of this work was that the electron path between the two electrodes could be very long due to the tendency of the magnetic field to force the electrons into circular orbits around the axis. In 1953 Wolfgang Paul in Bonn, investigated the non-magnetic quadrupole mass filter, which revolutionised mass spectrometry. His studies led to the development of the Paul or radiofrequency ion trap for the atomic ions. Since then various kinds of ion traps have been built which cater to specific investigations on the ions. Development of the Penning trap, using a dc electric field along with a magnetic field, was primarily by Hans Dehmelt and his associates in Seattle. Dehmelt trapped a single electron in a Penning trap by an electromagnetic potential. Dehmelt called this single electron bound to the gravitational field, the 'geonium atom'. The first atomic hyperfine structure experiment on trapped ions was performed by Dehmelt's group using the stored-ion exchange-collision technique in a Paul trap which paved the way for some of the subsequent experiment for atomic frequency

A single atom at rest in free space, free of uncontrolled perturbations, would be the ideal dream of any atomic physicist.



The purpose of an atom or ion trap is to confine the motion of the atomic or ionic particles to a small region of space.

standards. Confinement of charged particles made it possible to investigate some of the most fundamental properties of matter-radiation interaction. The immense impact of these studies was acknowledged in 1989 by the award of the Nobel Prize in Physics to Hans Dehmelt and Wolfgang Paul (half of the prize was awarded to Norman F Ramsay for introduction of oscillatory field in atomic-beam magnetic resonance method).

Confinement of Ions

The purpose of an atom or ion trap is to confine the motion of the atomic or ionic particles to a small region of space. In this article we discuss the trapping of charged particles, which is understandably far easier than the confinement of neutral atoms, as the forces which can be exerted by electromagnetic fields on the latter are far smaller.

How does one go about trapping an ion? The simplest solution is to have the ion elastically bound to an origin by a restoring force F that increases linearly with the distance r , $F = -kr$. In other words, if the ion moves back and forth about an equilibrium position through a parabolic potential Φ that varies as

$$\Phi = \frac{1}{2}kr^2 = \frac{1}{2}k(x^2 + y^2 + z^2), \quad (1)$$

then the particles are elastically bound to the origin. However, any potential in free space has to satisfy Laplace's equation $\nabla^2\Phi=0$; it can be shown that the above potential (1) does not. This is the essence of Earnshaw's theorem, which states that "A charged particle cannot be held in stable equilibrium by electrostatic forces alone" (see *Box 1*).

This necessitates a more involved arrangement if one wishes to trap the ions in three dimensions. Let us consider the electric quadrupole potential of the form

$$\Phi(x, y, z) = A(\alpha x^2 + \beta y^2 + \gamma z^2). \quad (2)$$



Box 1. Earnshaw's Theorem

Earnshaw's theorem states that it is not possible to arrange, in free space, charged particles in stable equilibrium. Let us consider the following arrangement in one dimension (*Figure A*), of a positive charge particle placed in between two negative charge particles. For this arrangement of charges to be in equilibrium, it can be worked out that the magnitude of the negatively charged particles has to be four times that of the positive charge placed at equi-distance 'a' from the two negative charges. This arrangement cannot be in a stable equilibrium, for even a slight displacement of any of the charges will render the entire system unstable. It is essentially a consequence of the fact that the potential $\phi(x)$ satisfying Laplace's equation $\nabla^2\phi = 0$ can have no maxima or minima.

The potential energies of each charge due to the other two can be easily worked out. For example the potential energy of the charge $-4q$ in the field of the other two charges is given by

$$W_{-4q} = -4q\left(\frac{q}{y} - \frac{4q}{a+y}\right) = 4q^2\left(\frac{3y-a}{y(a+y)}\right),$$

where y is the distance between the charge $+q$ and one of the displaced charges $-4q$. For $0 \leq y < \infty$, the potential energy between the charge $+q$ and the charge $-4q$ on the left side is shown by the curve ABC (*Figure A*), whereas for the other $-4q$ charge on the right for where $0 \geq y > -\infty$ the potential energy curve is shown by DEF. When the charges $-4q$ are stationary, the energy of the charge q is

$$W_q = q\left(\frac{-4q}{a-z} + \frac{4q}{a+z}\right) = \frac{-8q^2}{q^2 - z^2},$$

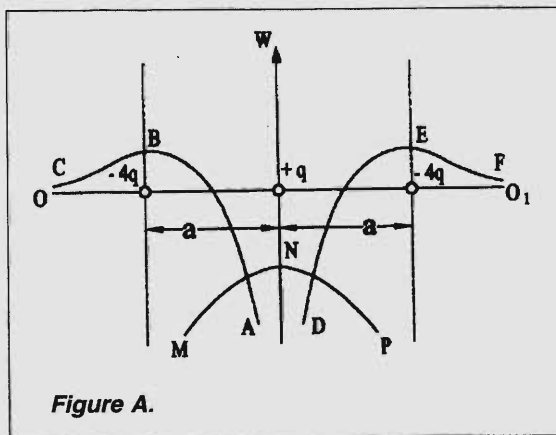


Figure A.

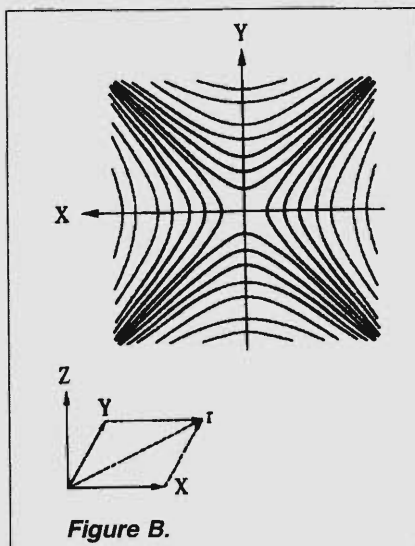


Figure B.

Box 1. continued...

where z is the displacement of the charge $+q$ from the equilibrium position. The potential energy curve of charge q for $0 \leq z \leq a$, is given by the curve MNP. It is interesting to note that the maxima of all three potential energy curves correspond to charges in equilibrium. It is for this reason that there is no stable equilibrium.

Earnshaw's theorem can be visualised in two dimensions (*Figure B*) by an arrangement consisting of a system of four hyperbolic electrodes, with adjacent electrodes oppositely charged as shown in *Figure 1*. The minimum distance between the opposite electrodes is $2\tau_0$. The solid lines in *Figure B* represent equipotential surfaces and the electric field centre is zero at the centre. A test charge placed at the centre would be at equilibrium, but not a stable one. While the zero potential of this point is a minimum with respect to the quadrants 1 and 3 it is a maximum with respect to quadrants 2 and 4. Such a point is called a saddle point. Thus charges cannot be in stable equilibrium in electrostatic fields alone.

The Laplace condition $\nabla^2 \Phi = 0$ imposes that the constants α , β and γ satisfy the condition $\alpha + \beta + \gamma = 0$. A simple way to satisfy this condition is by setting $\alpha = -\beta = 1$, $\gamma = 0$, which results in the two dimensional field

$$\Phi(x, y) = A\alpha(x^2 - y^2). \tag{3}$$

Figure 1. Electrode structure (of the two-dimensional mass filter) required to generate the potential given in (3).

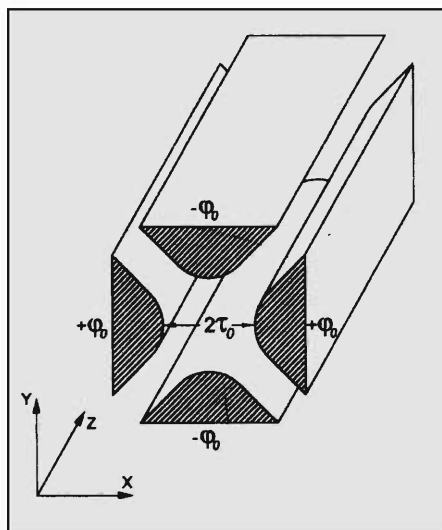
This potential can be generated by a set of four hyperbolically shaped electrodes separated by a distance $2\tau_0$ and linearly extended in z -direction, which is essentially the principle of the two-dimensional mass filter shown in *Figure 1*. The other possibility is by setting $\alpha = \beta$, $\gamma = -2\alpha$, which generates the three dimensional field

$$\Phi(x, y, z) = A\alpha(x^2 + y^2 - 2z^2), \tag{4}$$

the details of which will be discussed in the subsequent sections.

Three Dimensional Confinement

The three-dimensional quadrupole trap field given by (4) can be generated by a three-electrode structure as shown in *Figure 2*. There are two end-cap electrodes separated by a distance $2z_0$ and a ring electrode of radius r_0 , ($r_0 = 2z_0^2$) whose surfaces are hyperboloids of revolution about the z -axis.



For trapping the positive ions the two end-caps are held at a static positive potential with the ring electrode held at negative potential. Applying a potential U_0 between the end caps and the ring electrodes, (4) becomes

$$\Phi(x, y, z) = \frac{U_0}{2r_0^2} (2z^2 - x^2 - y^2), \quad (5)$$

where the field strength of this potential is given by

$$E_x = \left(\frac{U_0}{r_0^2} \right) x; \quad E_y = \left(\frac{U_0}{r_0^2} \right) y; \quad E_z = - \left(\frac{2U_0}{r_0^2} \right) z,$$

and for an ion of mass 'm', and charge 'q', we have

$$\frac{d^2 x}{dt^2} - \left(\frac{2qU_0}{mr_0^2} \right) x = 0 \quad (6a)$$

$$\frac{d^2 y}{dt^2} - \left(\frac{2qU_0}{mr_0^2} \right) y = 0 \quad (6b)$$

$$\frac{d^2 z}{dt^2} + \left(\frac{qU_0}{mr_0^2} \right) z = 0 \quad (6c)$$

Equation (6c) which represents a simple harmonic motion shows that the ion is trapped in a harmonic potential along the z -axis. However, the potential in the xy -plane defocuses the ions, which is of course consistent with Earnshaw's theorem as mentioned above. At the trap centre, the potential forms a saddle and the charged particles will be confined either in the radial plane or in the axial direction, but will escape in the other direction (*Figure 3*). In the Penning trap this is overcome by the addition of a magnetic field (*Figure 4a*), while in the Paul trap a RF potential is applied to the electrodes (*Figure 4b*).

The Penning Trap

It is now clear that, the dc field provides confinement of the ions along the axial direction while there is a repulsive force in the

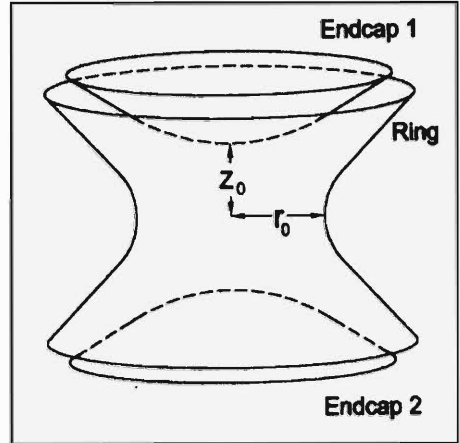


Figure 2. Electrode structure required to produce the three-dimensional rotationally symmetric quadrupole fields used in the ion trap.

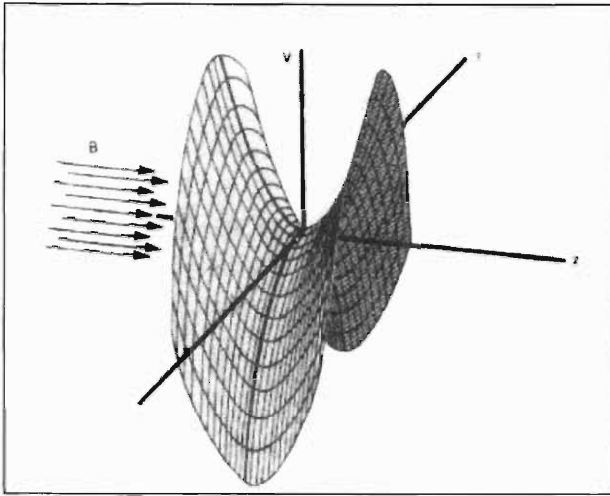


Figure 3. Equipotential surface (5) in an ion trap as a function of the axial co-ordinate z and the radial distance r . A positive ion starting from rest on the z -axis would oscillate along it, but any radial displacement would lead to instability. This can be prevented by alternating the potential in an RF (Paul) trap or adding a magnetic field B directed along the z -axis in the dc (Penning) trap.

radial xy -plane. Confinement of the ions in the Penning trap is achieved by adding a constant magnetic field B along the z -axis to the electrostatic field (Figure 4a). The three original translational degrees of freedom of the ion now become three modes of motion in the trap. The ion moving along the z -axis sees a parabolic potential,

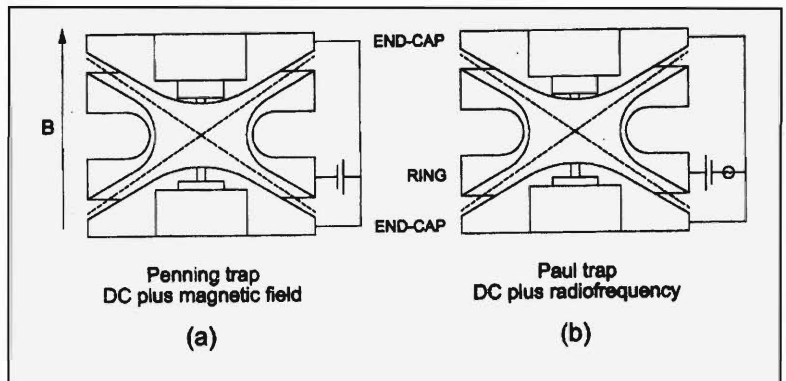
$$\Phi(x, y, z) = \frac{U_0}{2r_0^2} (2z^2 - x^2 - y^2) = \frac{U_0}{2r_0^2} (2z^2 - r^2) \tag{7}$$

and will undergo harmonic oscillations (6c) with a frequency ω_z (axial frequency),

$$\omega_z^2 = \frac{2qU_0}{mr_0^2} \tag{8}$$

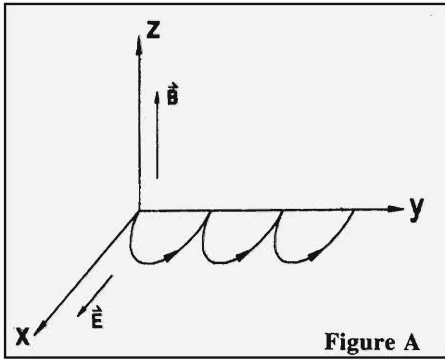
As the ion starts to escape along the radial plane, the magnetic field turns back the ion into a circular orbit (see Box 2). Thus in the radial plane the ion undergoes a circular motion with the centre at the origin. For this orbit, due to the radial component E_r , the electric force $qE_r = -q\partial\Phi/\partial r = qU_0/r/r_0^2$ almost balances the magnetic force qvB , that is $qU_0/r/r_0^2 = qvB$. Hence, the frequency of this circular motion ω_m , which is a constant of the

Figure 4. The cross-section of ion trap used in the (a) Penning and (b) Paul configurations.



Box 2. Cyclotron and Magnetron Motion

To understand the dynamics of the motion of the ion in the radial plane, let us first assume the presence of only the magnetic field B along the z -axis and the ion velocity in the radial plane. The ion in this case will undergo a cyclotron motion of frequency $\omega_c = qB/m$.



Next consider a constant electric field E in the x -direction. The ion will follow a cycloid motion in the radial plane, which can be described qualitatively as follows: Suppose initially the ion is at rest near the origin; the magnetic force is zero and the electric field accelerates it away from the centre in the x -direction. As the speed of the ion increases, the magnetic force increases which pulls the ion back towards the direction of y -axis as shown in *Figure A*. The faster it moves, the stronger the force due to the magnetic field which eventually turns the ion back to the y -axis, and as the ion is moving against the electric field, its speed decreases and eventually comes to zero on the y -axis. The entire process is periodically repeated and the ion slowly drifts away from the centre in the radial plane. This can be quantitatively worked out using the Lorentz force $\vec{F} = q(\vec{E} + \vec{v} \times \vec{B})$

In the ion trap the electric field in the x - y plane is radial. The slow drift motion, described in the above paragraph, is modified into a circular motion. This slow circular drift in the radial plane is called the *magnetron motion*.

In the ion trap the electric field in the x - y plane is radial. The slow drift motion, described in the above paragraph, is modified into a circular motion. This slow circular drift in the radial plane is called the *magnetron motion*.

trap, is given by

$$\omega_m = \frac{v}{r} = \frac{U_0}{r_0^2 B} \tag{9}$$

the cyclotron frequency ω_c given by,

$$\omega_c = \frac{qB}{m} \tag{10}$$

A more accurate analysis, taking into account the coupling of electric and magnetic fields, shows that the frequencies of cyclotron (ω_c) and magnetron motion (ω_m) (*Figure 5*) are slightly modified

$$\omega_c = \frac{1}{2} \omega_c + \left(\frac{\omega_c^2}{4} + \frac{\omega_z^2}{2} \right)^{1/2} \tag{11}$$



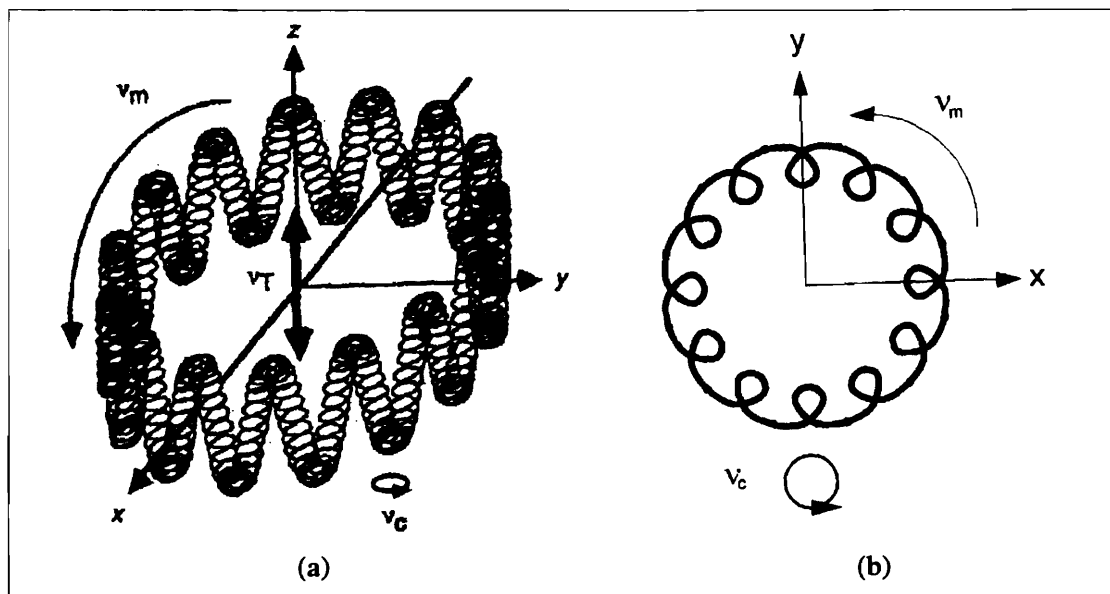


Figure 5. Ion trajectory (left) in an ion trap, with all three fundamental modes (cyclotron $\omega_c = 2\pi\nu_c$, magnetron $\omega_m = 2\pi\nu_m$ and axial $\omega_z = 2\pi\nu_z$ excited, and the projections (right) of that trajectory onto the xy plane.

$$\omega_m = \frac{1}{2} \dot{\nu}_c - \left(\frac{\dot{\nu}_c^2}{4} + \frac{\dot{\nu}_z^2}{2} \right)^{1/2} \quad (12)$$

Confinement is assured if the action of the magnetic field exceeds the defocusing force of the electric field. In order to obtain stable orbits, we must have real values for ω'_c and ω'_m . that is,

$$\frac{\dot{\nu}_c^2}{2} > \dot{\nu}_z^2 \quad (13)$$

is the condition for stability in the Penning trap.

The Paul Trap

In a Paul trap, an oscillating electric potential is applied between the ring and the two end-cap electrodes (Figure 4b) in conjunction with the static electric potential U_0 . The trap potential then has the form

$$\Phi(x, y, z) = \left(\frac{U_0 - V_0 \cos(\Omega t)}{2r_0^2} \right) (x^2 + y^2 - 2z^2), \quad (14)$$

where V_0 and Ω are the amplitude and frequency, respectively of the oscillating electric potential.

The trap is stable in the axial direction and unstable in the radial plane for half the cycle and vice versa for the next half of the cycle. However, owing to the field inhomogeneity, the force averaged over a period of the oscillating field does not average to zero but is directed towards the regions of weak field, that is, towards the trap centre. At the trap centre, there is no field variation; therefore there is no motion due to the RF field and ideally a particle set at the trap centre would remain at rest.

The equation of motion for a particle of mass m and charge q is

$$\frac{d^2}{dt^2} \begin{pmatrix} x \\ y \\ z \end{pmatrix} + \frac{e}{mr_0^2} [U_0 - V_0 \cos(\Omega t)] \begin{pmatrix} x \\ y \\ -2z \end{pmatrix} = 0. \quad (15)$$

If the following substitutions are made,

$$a = \frac{8eU}{mr_0^2 \Omega^2}; \quad q = \frac{4eV_0}{mr_0^2 \Omega^2}; \quad \tau = \frac{1}{2} \Omega t, \quad (16)$$

then we obtain the following set of Mathieu equations

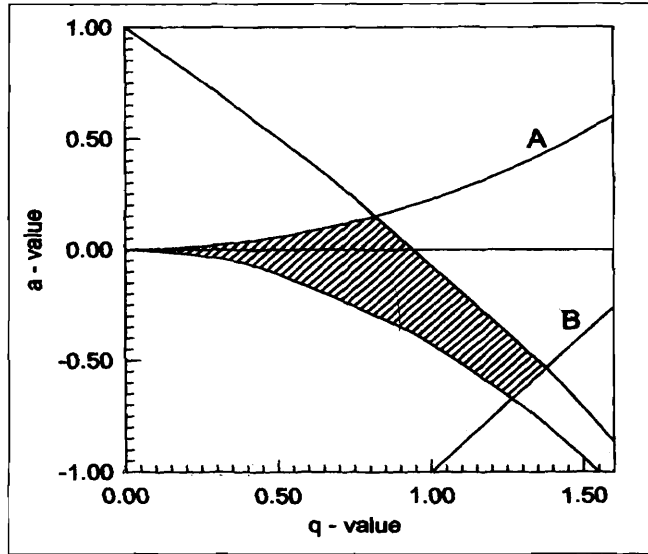
$$\frac{d^2}{dt^2} \begin{pmatrix} x \\ y \\ z \end{pmatrix} + [a - 2q \cos(2\Omega t)] \begin{pmatrix} x \\ y \\ -2z \end{pmatrix} = 0. \quad (17)$$

It has been shown that (17) possesses bounded (stable) and unbounded (unstable) solutions depending on the values of 'a' and 'q'. Figure 6 shows a section of the a - q stability plane for certain values of a and q . In the range of a and q shown here, the stable motion is encountered only in the regions A and B, whereas all the other displayed a - q combinations will lead to unbounded motion.

In general the solution of the equations of motion (17) is complicated but, when $a \ll q \ll 1$, an approximate solution can be



Figure 6. A section of the Mathieu stability diagram for the Paul trap. The motion is simultaneously stable both in the axial and radial directions only within the shaded regions.



found. In this case the motion reduces to

$$\begin{aligned}
 x_i(t) &= x_{i0} \left[1 + \frac{\beta_i}{2} \cos(\Omega t) \right] \cos(\omega_i t) \\
 &= x_{i0} \left\{ \cos(\omega_i t) + \frac{\beta_i}{4} \cos[(\Omega + \omega_i)t] + \frac{\beta_i}{4} \cos[(\Omega - \omega_i)t] \right\}
 \end{aligned}
 \tag{18}$$

$$\dot{u}_i = \frac{\beta_i \Omega}{2} ; \beta_i = a_i + \frac{1}{2} q_i^2 \approx \frac{1}{2} q_i^2
 \tag{19}$$

We see that, for $a \ll q \ll 1$, the motion can be easily demonstrated in a mechanical analogue device. In the quadrupole trap the equipotential lines form a saddle surface. Such a surface can be machined and mounted on a platform, which can be rotated, as shown in *Figure 3*. If one puts a small steel ball on it, then it will roll down; that is, its position is unstable. However, if one rotates the platform with the right frequency appropriate to the potential parameters and the mass of the ball, the ball becomes stable, makes small oscillations, and can be kept in that stable position for a long time. If one adds a second or a third ball, these balls also stay stable near the centre of the disc.



Some Applications of Ion Traps

The unique and important features of ion trapping techniques are:

- Storage of charged particles in a very well controlled environment nearly free of unwanted perturbations enables the highly precise and accurate measurement of interaction constants, as the transit-time line broadening is nearly eliminated (see *Box 3*).
- Extreme reduction of Doppler broadening can be achieved, due to the possibility of very effective cooling of the trapped ions. Several cooling techniques have been developed in order to reduce the kinetic energies, thereby minimising the first order as well as the second-order Doppler effects and localising the charged particles near the trap centre, thereby achieving very high resolution and accuracy in the spectroscopic measurements.
- The possibility of performing experiments on few ions or even a single ion reduces or eliminates the ion-ion Coulomb interactions and thus very rare species like anti-proton, positron, short-lived isotopes or exotic particles like C_{60} , can be investigated.
- Ion traps are now routinely being used as a mass spectrometer. Highest mass resolving power and accuracy are obtained by Penning traps. Mass spectrometers based on Penning traps have been used for the accurate mass measurements of anti-protons, mass of light ions and, recently, measurements of mass of heavy ions.

As mentioned above ion traps find numerous applications in the field of high-resolution optical double resonance spectroscopy, single-ion spectroscopy, precision mass measurements of stable and radioactive isotopes, atomic frequency standards, and some of these are briefly discussed below.

(a) Optical RF – Double Resonance Spectroscopy: The conventional techniques of high resolution spectroscopy are limited by large Doppler widths (see *Box 3*) of spectral lines, typically of the

Extreme reduction of Doppler broadening can be achieved, due to the possibility of very effective cooling of the trapped ions.



Box 3. Line Broadening Mechanism

Spectral lines in discrete absorption or emission spectra are never strictly monochromatic. Even with very high resolution one observes a spectral distribution $I(\omega)$ of the observed or emitted intensity around the central frequency $\omega_0 = (E_f - E_i)/\hbar$ corresponding to an atomic transition between upper level E_f and lower level E_i . Some of the broadening mechanisms of spectral lines are discussed below.

Natural Linewidth: If τ is the mean lifetime of an energy level E then according to the uncertainty principle its energy E can be determined only with an uncertainty $\Delta E = \hbar/\tau$. This results in the total uncertainty

$$\Delta E = \Delta E_i + \Delta E_f = \hbar \left(\frac{1}{\tau_i} + \frac{1}{\tau_f} \right),$$

which leads to the natural line broadening of a spectral transition

$$\Delta \omega = \frac{\Delta E}{\hbar} = \left(\frac{1}{\tau_i} + \frac{1}{\tau_f} \right).$$

Doppler Linewidth: The Doppler width arises due to the thermal motion of atoms absorbing or emitting radiation. Suppose that an atom in the excited energy levels E_f moving with a velocity \vec{v}_f emits a photon of energy $\hbar\omega$ and momentum $\hbar\vec{k}$, resulting in the transition $E_f \rightarrow E_i$ where E_i is the lower energy level. The emission of radiation causes the atom to recoil to a new velocity \vec{v}_i . Conservation of momentum demands, that

$$M\vec{v}_f = M\vec{v}_i + \hbar\vec{k}, \quad (1)$$

where M is the mass of the atom. Energy conservation under non-relativistic conditions is

$$E_f + \frac{1}{2}Mv_f^2 = E_i + \frac{1}{2}Mv_i^2 + \hbar\omega. \quad (2)$$

If ω_0 is the frequency of light, which would be emitted if the atom had zero velocity before and after the emission, then

$$\hbar\omega_0 = E_f - E_i. \quad (3)$$

Elimination of \vec{v}_f , E_i , E_f from (3) with use of (1) and (2) gives,

$$\dot{\omega} = \omega_0 + \vec{k} \cdot \vec{v}_i - \frac{\hbar k^2}{2M} = \omega_0 + \frac{\omega v_i}{c} - \frac{\hbar \omega^2}{2Mc^2}. \quad (4)$$

The second term is the linear (first-order) Doppler effect describing the well-known $\Delta\dot{\omega} = \vec{k} \cdot \vec{v}$ Doppler shift. Thus the width can be reduced by making observations perpendicular to the emitting atoms,

Box 3. continued...

Box 3. continued...

as in experiments with collimated atomic beams. The third term in (4) is the photon recoil effect. Typical orders of magnitude for some quantities on the right of (4) are $\frac{v}{c} \approx 10^{-5}$, $\frac{\hbar\omega}{2Mc^2} \approx 10^{-9}$. Although the first order Doppler width can be completely eliminated by using various techniques, the second order Doppler effect, which is purely relativistic, persists.

Consider an atom (modelled as an oscillator) travelling along the z -axis. We observe the emission say along the x -direction. If the period of the stationary oscillator (atom) is τ_0 then the period in the laboratory

frame is $\tau = \tau_0 \left(1 - \frac{v^2}{c^2}\right)^{1/2}$, due to time dilation. Hence the frequency of emission $\omega = 2\pi/\tau$ will be,

$$\omega = \omega_0 \left(1 - \frac{v^2}{c^2}\right)^{1/2} \approx \omega_0 - \frac{\omega_0 v^2}{2c^2}.$$

The second term here is the second order Doppler effect. Note that this term is independent of the direction of \vec{v} and can be eliminated only by making $\vec{v} = 0$.

Transit-Time Broadening: If the interaction time of atoms with the radiation field is small compared with the spontaneous lifetime of the excited level, then it leads to transit-time or time-of-flight broadening. Consider an atom interacting with monochromatic light of frequency ω during the interval T . The atom experiences the following field

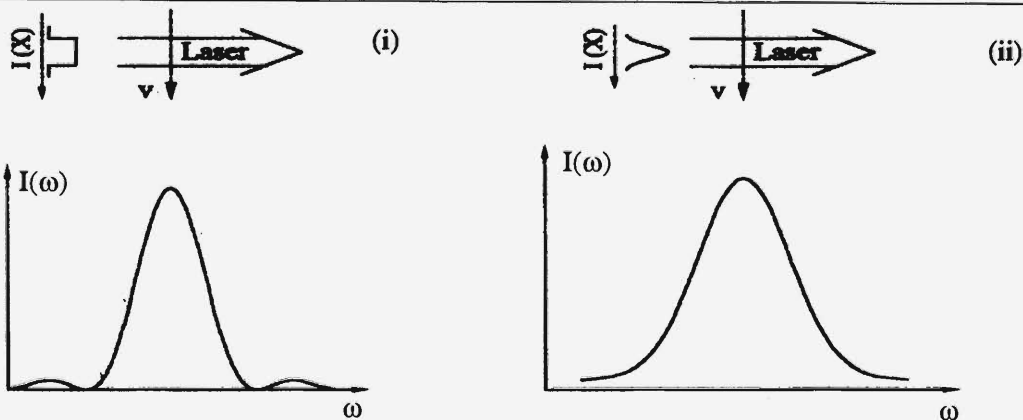
$$E(t) = A_0 \cos(\omega_0 t) \quad 0 \leq t \leq T$$

$$= 0 \quad t > T$$

which in the frequency domain is obtained from the Fourier transform

$$E(\omega) \equiv \frac{1}{\sqrt{2\pi}} \int_0^T A_0 \cos(\omega_0 t) e^{-i\omega t} dt$$

Figure A



Box 3. continued...

Box 3. continued...

The intensity profile of the spectral line, $I(\omega) = E^*(\omega)E(\omega)$ is, for $(\omega - \omega_0) \ll \omega$,

$$I(\omega) = C \frac{\sin^2 [(\omega - \omega_0)T / 2]}{(\omega - \omega_0)^2},$$

where C is a constant. This is a function with a full half-width $\delta\omega_r = 5.6 / T$ (see *Figure A*). The intensity profile of the spectral line is shown for, (i) rectangular and (ii) Gaussian laser pulses. For a beam of fast ions with typical velocity 3×10^8 cm/sec, the time required to traverse a laser beam of width 0.1 cm is less than 10^{-9} sec which is shorter than the spontaneous lifetimes of most atomic levels. With $T \approx 10^{-9}$ sec, the full-width at half maximum of the transit time broadening $\omega_r \approx 10^9$ Hz.

order of $0.05 \text{ cm}^{-1} \approx 1500 \text{ MHz}$. These optical techniques are incapable of achieving the required resolution and precision for measuring small splitting/shifts in the energy levels. This is mainly due to the fact that a small energy separation is being measured indirectly by taking the difference between two very large optical frequencies.

In double resonance spectroscopy two electromagnetic fields of different frequencies are simultaneously in resonance with two atomic or molecular transitions sharing a common energy level. The first electromagnetic field takes the atoms/molecules to an excited state and the second field, which could be in the RF or microwave region, induces transitions between energy levels which are very closely spaced. As the transition is taking place in the RF region, the Doppler line width is reduced.

Further more in a trap the ion motion is restricted to amplitudes which are small compared to the wavelength of the microwave radiation. Thus there is no first-order Doppler effect and in addition there is elimination of the time-of-flight broadening, allowing high-resolution optical double resonance spectroscopy to be performed. Using this technique very high resolution and accuracy has been achieved, e.g. a line width of 2 mHz (millihertz) has been obtained.

(b) Single Ion Spectroscopy: Ion traps make it possible to study a single cold ion, and the use of laser cooling techniques further



removes all orders of Doppler effects on the atomic transitions. Thus a series of experiments in basic physics have been performed, such as observation of quantum jumps, experimental test of quantum Zeno effect, a precision test of the linearity of quantum mechanics and so on. E Peik and others (1994) have performed laser cooling and quantum jumps on a single Indium ion. For a single ion they observed quantum jumps and out of the 3P_0 level. Quantum Zeno effect was experimentally tested by Itano and others (1990) with atomic level measurements realised by means of a short laser pulse.

(c) **Precision Mass Measurement:** Very precise values of g -factors and mass ratios have been obtained by measuring ion oscillation frequency in a Penning trap. As shown in (7-11), the motional frequencies in Penning traps are related to cyclotron frequency $\omega_c = eB/m$ and the basic idea for g -factor and mass measurements is a precise determination of the cyclotron frequency of the trapped particles.

The apparatus set up at the ISOLDE facility at European Centre for Nuclear Research, Geneva for the direct measurement of masses of radioactive isotopes uses ions delivered by the online separator and involves two Penning traps arranged in tandem. Kluge and others (1993) have measured the masses of unstable isotopes (^{142}Cs $t_{1/2} \sim 1.8\text{sec}$) with a measurement accuracy of $\delta m/m \approx 10^{-7}$ and resolving power $m/\Delta m \approx 10^6$.

(d) **Frequency Standards:** The most important possible application of cooled-trapped ions is the development of trapped ion frequency standards for both optical and microwaves regions. Ion traps offer the potential for achieving cooled ion species with very narrow resonances (with line widths a fraction of a Hertz, both in optical and microwave regions) with high accuracy and stability. A variant of the quadrupole trap capable of localising a trapped ion within much less than an optical wavelength has been realised by S R Jefferts, C Monroe and D J Wineland (1995).

Suggested Reading

- [1] E Peik, G Hollemann and H Walther, Laser cooling and quantum jumps of a single Indium ion, *Phys. Rev., A* 49, 402, 1994.
- [2] W M Itano and others, Quantum Zeno effect, *Physics Rev., A* 41, 2295, 1990.
- [3] G Bollen and others, High accuracy mass determination of unstable Rb, Sr, Cs, Ba, Fr and Ra isotopes with a Penning trap mass spectrometer, Nuclear shapes and nuclear structure at low excitation energies, *Proceedings of a NATO Advanced Research Workshop*, p. 399-405, 1993.
- [4] S R Jefferts, C Monroe and D J Wineland, Coaxial resonator driven RF (Paul) trap for strong confinement, *Phys. Rev., A* 51, 3112, 1995.

Address for Correspondence
 Pushpa M Rao, Richard D'Souza
 and S A Ahmad
 Spectroscopy Division
 Bhabha Atomic Research Centre
 Trombay
 Mumbai 400 085, India.

